Semiclassical Transport Models for Semiconductor Spintronics

Yuriy V. Pershin,[1,2] **Semion Saikin**[1,3] **and Vladimir Privman**[1]

[1] *Center for Quantum Device Technology, Clarkson University, Potsdam, NY 13699-5721, USA*

[2] *Department of Physics and Astronomy, Michigan State University, East Lansing, Michigan 48824-2320, USA*

[3] *Department of Theoretical Physics, Kazan State University, Kazan 420008, Russia*

ABSTRACT

We overview and consider several examples of applications of semiclassical approaches used in semiconductor spintronic device modeling. These include drift-diffusion models, kinetic transport equations and Monte Carlo simulation schemes.

I. INTRODUCTION

Recent advances [1–6] in experimental studies of spin polarized transport in semiconductor structures have moved the state of the art closer to the realization of novel spintronic devices. It is expected [7] that utilization of spin-related phenomena will extend the functionality of conventional devices at the classical level and address fundamental problems of electronics in the quantum limit [1–6]. Different types of semiconductor and hybrid spintronic devices [8–20] have been proposed. Spintronic devices allow control of functionality by spin-orbit and magnetic interactions and can be used as magnetic sensors or programmable logic elements. In comparison with metal-based spintronics, reviewed in [21], utilization of semiconductor structures promises more versatile applications due to ability to adjust potential variation and spin polarization in the device channel by external voltages, device geometry and doping profiles. Moreover, semiconductor spintronic devices will be compatible with conventional circuitry [4]. According to a more skeptic view semiconductor spintronic devices will be limited to several specific applications [22, 23].

In general, transport in semiconductor spintronic devices can be characterized by the creation of a non-equilibrium spin polarization in the device (spin injection), measurement of the final spin state (spin detection), external control of spin dynamics by the electric (gate modulation) or magnetic fields, and uncontrolled spin dynamics leading to loss of information in the device (spin relaxation or spin dissipation). The role of spintronic device modeling has been to evaluate whether spin polarization control is applicable for devices at the present and near-future stages of semiconductor technology, and how can the spin be controlled most efficiently.

Recent experimental advances have demonstrated that the spin polarization can be maintained for up to nanoseconds at room temperature in GaAs(110) quantum wells [24]. Efficient gate control for spin relaxation in a similar structure has been reported [25]. Coherent injection of polarized spins across material interfaces [26] and coherent transport of spin polarization in homogeneous materials for a distance longer than 100 micrometers [27] have been studied by optical techniques at low temperatures. Pure spin currents without charge transport have been created using two-color laser pumping [28]. These results represent a small fraction of the recent experimental achievements [2].

Once injected into a semiconductor, electrons experience spin-dependent interactions with the environment, which cause relaxation. The following spin-dependent interactions can be identified: external magnetic fields, pairwise magnetic interactions of the electrons, spin-orbit interactions, exchange interactions, hyperfine interactions with nuclear spins [22]. In many experimental situations the spin-orbit interactions are important. Many spintronic devices utilizing spin-orbit interaction in semiconductor heterostructures for spin control and manipulation [8, 10, 11, 13–15] have been proposed.

There are two main types of spin-orbit interaction in semiconductor heterostructures. The Dresselhaus spin-orbit interaction [29] appears as a result of the asymmetry present in certain crystal lattices, e.g., zinc blende structures. The Rashba spin-orbit interaction [30] arises due to the asymmetry associated with the confinement potential and is of interest because of the ability to electrically control the strength of this interaction. The latter is utilized, for instance, in the seminal spintronic design of an electro-optic modulator proposed by Datta and Das [8].

The Hamiltonian for the Rashba interaction is written [30] as

$$H_R = \alpha \hbar^{-1} \left(\sigma_x p_y - \sigma_y p_x \right), \tag{1}$$

where α is the interaction constant, σ is the Pauli-matrix vector corresponding

to the electron spin, and $\mathbf{p}$ is the momentum of the electron confined in a two-dimensional geometry. For two-dimensional heterostructures with appropriate growth geometry, the Dresselhaus spin-orbit interaction is of the form [29]

$$H_D = \beta\hbar^{-1}\left(\sigma_y p_y - \sigma_x p_x\right), \tag{2}$$

where β is the interaction constant. The prime objective of spintronic device modeling is incorporation of the spin degree of freedom, as well as spin-dependent interactions, into the transport simulation schemes.

The main purpose of this paper is to present different approaches used in modern scientific investigations of spin-related processes in semiconductor structures. Modeling of different level of complexity and accuracy will be surveyed. The hierarchy of theoretical models for spin-polarized transport involves drift-diffusion models, kinetic transport equations, and Monte Carlo simulation schemes. Drift-diffusion approximations allow reasonably simple and transparent description of physical phenomena and are valid within a wide range of experimental parameters, e.g., temperature, field magnitude, etc. Usually the parameters used in drift-diffusion approximations could be obtained from kinetic transport models or by Monte Carlo simulations.

Our paper is organized as follows. In Sec. II we introduce drift-diffusion approximations for spin-polarized transport. Our attention is focused on the two-component drift-diffusion approximations and spin-polarization-vector-based drift-diffusion models. Sec. III is devoted to kinetic transport equations describing spin-polarized transport. Monte Carlo simulation schemes are presented in Sec. IV. Applications of the discussed approaches to spin-polarized transport are given throughout the text. They are based primarily on the works by the authors. Readers interested in a broader overview of semiconductor spintronics should consult the recent comprehensive review article by Žutić et al. [2].

II. DRIFT-DIFFUSION APPROXIMATION

The drift-diffusion approximation does not requires large computational resources and is probably the most simple and straightforward method for spin-involving process modeling. It is possible to classify the existing drift-diffusion schemes for spin polarized transport into two main approaches differently accounting the spin degree of freedom. These are the two-component drift-diffusion model and spin-polarization-vector or density-matrix based approximations. Both models have been successfully used in practical modeling of spin-related phenomena in semiconductors in the last few years [31–43]. General

conditions for the applicability of these approximations are not different from the usual conditions of applicability of drift-diffusion approximations. We will present here only those drift-diffusion approximations neglecting the influence of spin on the electron spatial motion. An example of a drift-diffusion scheme incorporating the latter effect can be found in [42].

A. Two-component model

1. Model description

Within the two-component drift-diffusion model, the electrons in a semiconductor are considered to be of two types, namely, having spins up or down. This is usually applicable on the timescale much large than the transverse spin dephasing/decoherence time. Such models have been developed first for spin transport in ferromagnetic metals [43, 44], including the effects of doping and electric field [31–33, 45].

Each type of electron is described by the usual set of drift-diffusion equations with additional terms related to sources and relaxation of the electron spin polarization. Usually, the mechanism of the spin relaxation is not specified in such kind of models. All information about the spin relaxation is contained in the single parameter—the electron spin relaxation time τ_{sf}. The set of equations for the spin-up and spin-down electrons has the following form,

$$e\frac{\partial n_{\uparrow(\downarrow)}}{\partial t} = \mathrm{div}\mathbf{j}_{\uparrow(\downarrow)} + \frac{e}{2\tau_{sf}}\left(n_{\downarrow(\uparrow)} - n_{\uparrow(\downarrow)}\right) + S_{\uparrow(\downarrow)}\left(\mathbf{r},t\right), \tag{3}$$

$$\mathbf{j}_{\uparrow(\downarrow)} = \sigma_{\uparrow(\downarrow)}\mathbf{E} + eD\nabla n_{\uparrow(\downarrow)}, \tag{4}$$

$$\mathrm{div}\mathbf{E} = \frac{e}{\varepsilon\varepsilon_0}\left(N - n\right), \tag{5}$$

where $-e$ is the electron charge, $n_{\uparrow(\downarrow)}$ is the density of the spin-up (spin-down) electrons, $\mathbf{j}_{\uparrow(\downarrow)}$ is the current density, $S_{\uparrow(\downarrow)}\left(\mathbf{r},t\right)$ describes the source of the spin polarization, $\sigma_{\uparrow(\downarrow)} = en_{\uparrow(\downarrow)}\mu$ is the conductivity, μ is the mobility, connected with the diffusion coefficient D via the Einstein relation $\mu = De/(k_BT)$, and defined via $\mathbf{v}_{\mathrm{drift}} = \mu\mathbf{E}$, N is the positive background charge density and $n = n_\uparrow + n_\downarrow$ is the charge density, ε_0 is the permittivity of free space, and ε is the dielectric constant. Equation (3) is the usual continuity relation that takes into account spin relaxation and sources of the spin polarization, Eq. (4) is the expression for

the current which includes the drift and diffusion contributions, and Eq. (5) is the Poisson equation. It is assumed here that the diffusion coefficient and the spin relaxation time are equal for spin-up and spin-down electrons.

To separate the equations for the charge and spin degrees of freedom, it is convenient to introduce the spin polarization density $P = n_\uparrow - n_\downarrow$. Then, the following equation for P in 1D can be obtained from Eqs. (3) and (4),

$$e\frac{\partial P}{\partial t} = D\Delta P + D\frac{e\mathbf{E}}{k_B T}\nabla P + D\frac{e\nabla\mathbf{E}}{k_B T}P - \frac{P}{\tau_{sf}} + F(\mathbf{r},t)\,. \tag{6}$$

Here $F(\mathbf{r},t) = [S_\uparrow - S_\downarrow]/e$ represents a spin polarization density created by the external source. The spin polarization density is coupled to the charge density through the electric field. Equation for the electric field can also be found from the set (3)-(5); for details see [33]. Thus, finding a solution involves two steps: first, the electric field profile is calculated and, second, Eq. (6) is solved for the spin polarization density. Moreover, it should be mentioned that in real calculations the current, rather than the applied voltage, is more convenient as the external control parameter, because it is constant throughout the electric circuit that contains the sample. If we use the voltage as the external control parameter, then it is necessary to take into account voltage drops in different parts of the circuit, such as, for example, at the Schottky barriers between metal and semiconductor.

2. Focusing of electron spin polarization by inhomogeneous doping

The two-component drift-diffusion approximation was used in studies of propagation of spin-polarized electrons through a semiconductor region with variable level of doping ($n - n^+$ junction) [33, 34]. The system under investigation and a selected result are shown in Fig. 1. It is assumed that a localized source of spin-polarized electrons is located in the low-doped region with the doping level N_1. The injection from the source results in a difference in concentrations of electrons with opposite spin direction. Under influence of the electric field, the non-equilibrium spin polarization drifts in the direction of the high-doped region N_2.

The two-component drift-diffusion model was used in calculations of the electric field distribution and spin polarization distribution. We have obtained an interesting result concerning propagation of spin-polarized current through a boundary between two semiconductor regions with different doping levels. It was found that the spin polarization density can be condensed and amplified near the

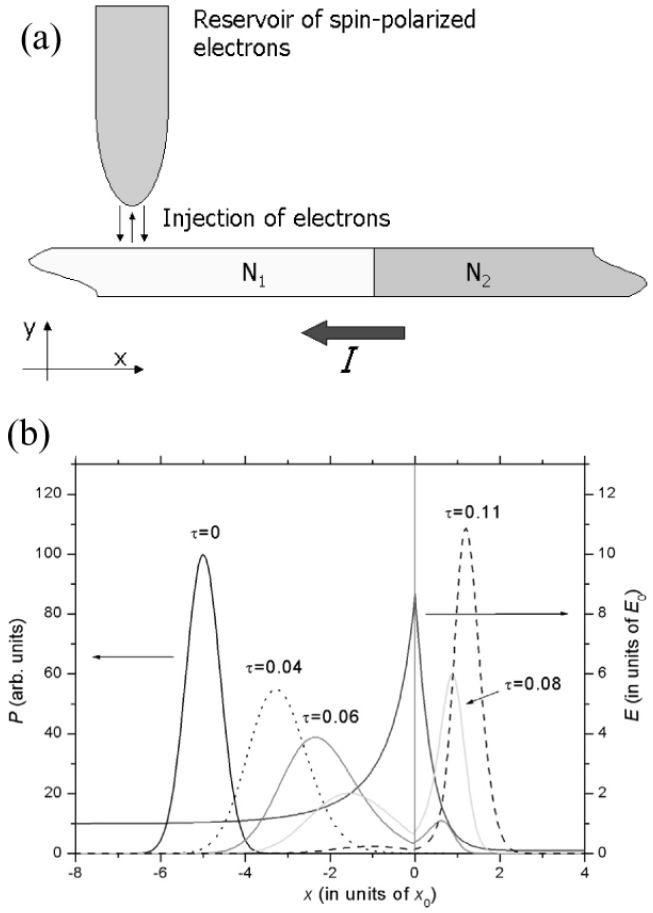

FIG. 1: (a) Schematic representation of the system. Spin-polarized electrons are injected into the low-doped region. (b) Dynamics of propagation of spin-polarized electrons, injected at $t = 0$, through the boundary. The curve peaked at $x = 0$ denotes the electric field. The other curves show the spin polarization density at several times.

boundary; see Fig. 1(b). The built-in electric field at the boundary accelerates propagation of the spin polarization through the boundary, if spin polarization passes from the low-doped region to high-doped region. Spin amplification occurs past the boundary, within the distance of the order of the depletion layer width. We point out that this mechanism, involving only the doping variation, has the advantage of not requiring a materials interface, thus avoiding additional spin polarization losses.

Propagation of spin-polarized electrons through a boundary between two different semiconductors was also considered [35]. An analytic formula describing the rate of spin accumulation on the boundary was derived. It was shown that

the amplitude of the electron spin polarization at the boundary increases with increase of the doping level and spin relaxation time, and with decrease of the diffusion coefficient of the second semiconductor.

3. Gate control for spin polarization drag

The described approach can be applied to device modeling in the case of only two spin states playing a role in device operation [14, 16, 17]. For example, it can be used to study gate modulation of the spin relaxation rate in non-ballistic spin-FET [14]. Such a device utilizes the interference between the Rashba (1) and Dresselhaus (2) interactions in the device channel, that is formed at a semiconductor heterostructure interface. If the coupling coefficients α and β are equal, the spin dephasing is suppressed, as described in more detail in the next section. In the leading order of approximation, electrons injected with spin along the z-axis remain spin-polarized during their motion along the device channel. If the spin-orbit coefficients are made not equal, then electron spin polarization decreases. This can be controlled by the gate voltage, because both spin-orbit coupling coefficients are dependent on the electric field orthogonal to the device channel. Spin filtering at the drain (using magnetic contact, for example) will modulate current through the device depending on the spin polarization. Transport of spin density along the channel in this case (an electron density is constant) is described by the exponential decay function [37]

$$P(x) = P(0)e^{-x/L_{\mathrm{s}}}, \tag{7}$$

with the characteristic spin scattering length

$$L_{\mathrm{s}} = \left(\frac{\mu E}{2D} + \sqrt{\left(\frac{\mu E}{2D} \right)^2 + \left(\frac{2m^*(\alpha - \beta)}{\hbar^2} \right)^2} \right)^{-1}. \tag{8}$$

Using rather sophisticated procedure for calculation of the spin-orbit coupling constants, α and β, as functions of the gate voltage, it is possible to deduce that modulation of the spin polarization drag can be observed at room temperature in a submicron size device within a reasonable range of the gate voltage [38].

B. Spin polarization vector approach

1. Method

This approach allows accounting for transverse spin dynamics of carriers [37, 39, 40, 42] as an extension of the previously discussed model. Such description is important for systems with small energy gap between the spin-up and spin-down states, when the spin dephasing time is appreciably longer than the time scales of the processes studied. Utilization of coherent spin dynamics opens a way for analogue magnetoelectronic devices [48]. The spin polarization density, $\mathbf{P}$, in this case is a vector quantity. It can be obtained from a single-particle spin density matrix,

$$\rho = \begin{pmatrix} \rho_{\uparrow\uparrow} & \rho_{\uparrow\downarrow} \\ \rho_{\downarrow\uparrow} & \rho_{\downarrow\downarrow} \end{pmatrix}, \tag{9}$$

where the matrix elements are parameterized by components of the spin polarization vector,

$$\begin{aligned} \rho_{\uparrow\uparrow,\downarrow\downarrow} &= (1 \pm P_z)/2, \\ \rho_{\uparrow\downarrow,\uparrow\downarrow} &= (P_x \mp iP_y)/2. \end{aligned} \tag{10}$$

It should be noted that such representation is still a single-electron description. For example, it cannot describe spin entanglement of two electrons. Under assumption that the spin degree of freedom does not affect the spatial motion, it is possible to show that the dynamics of $\mathbf{P}$ is described by a vector drift-diffusion equation. In the 1D case, we have

$$\frac{\partial \mathbf{P}}{\partial t} + \hat{\mathbf{D}}\frac{\partial^2 \mathbf{P}}{\partial x^2} + \hat{\mathbf{A}}\frac{\partial \mathbf{P}}{\partial x} + \hat{\mathbf{C}}\mathbf{P} = 0. \tag{11}$$

The coefficients $\hat{\mathbf{D}}, \hat{\mathbf{A}}, \hat{\mathbf{C}}$, in Eq. (11) are 3 by 3 matrixes. The symmetry of these coefficients is defined by the properties of specific spin-dependent interactions. In general, all three matrix coefficients cannot be diagonalized simultaneously and equations for the components of spin polarization density vector cannot be decoupled. Equation (11) can be derived by different methods. For example, it was obtained from kinetic transport equations using the moment expansion procedure [37] and from general stochastic principles [40].

2. Short-time approximation

In many applications, it is important to find the space distribution of the spin polarization $\mathbf{P}(\mathbf{r},t)$ at an arbitrary moment of time t, given the initial spin polarization distribution $\mathbf{P}(\mathbf{r},t=0)$. Initial dynamics of spin polarization distribution can be found using the short-time approximation [41]. Within this approximation $\mathbf{P}(\mathbf{r},t)$ in 2DEG geometry is given by

$$\mathbf{P}(x,y,t)=\int\int G(x-x',y-y',t)\mathbf{P'}_{(x,y),(x',y')}dy'dx', \tag{12}$$

where $G(x-x',y-y',t)$ is the diffusion Green function (solution of a diffusion equation with a point source), and $\mathbf{P'}_{(x,y),(x',y')}$ represents a contribution of the initial spin polarization density at point (x',y') to $\mathbf{P}(x,y,t)$. The structure of Eq. (12) can be easily understood. Electron spin polarization density in a space volume with coordinates (x,y) at a selected moment of time t is given by a sum of spin polarization vectors of all electrons located in this volume. The diffusion Green function $G(x-x',y-y',t)$ gives the probability for the electrons to diffuse from the point (x',y') to (x,y), while $\mathbf{P'}_{(x,y),(x',y')}$ describes the spin polarization of these electrons.

We note that Eq. (12) governs only the initial spin relaxation dynamics. The main approximation is the assumption that different spin rotations commute with each other, and the spin precession angle φ is proportional to the distance between (x',y') and (x,y). This assumption is justified when the spin precession angle per mean free path is small and the time is short. Moreover, it is assumed that evolution of the electron spin degree of freedom is superimposed on the space motion of the charge carriers. In other words, the influence of the spin-orbit interaction on the spatial motion is neglected. If $\mathbf{a}$ is the unit vector along the precession axis, then [40]

$$\mathbf{P'}_{(x,y),(x',y')}=\mathbf{P}+\mathbf{P}_{\perp}\left(\cos\varphi-1\right)+\mathbf{a}\times\mathbf{P}\sin\varphi, \tag{13}$$

where $\mathbf{P}_{\perp}=\mathbf{P}-\mathbf{a}(\mathbf{aP})$ is the component of the spin polarization perpendicular to the precession axis, $\varphi=\eta r$, η is the spin precession angle per unit length, $\mathbf{r}=(x-x',y-y')$, $r=|\mathbf{r}|$. Here $\mathbf{P}\equiv\mathbf{P}(\mathbf{r},t=0)$. In 2DEG with only Rashba spin-orbit interaction, $\mathbf{a}=\hat{z}\times\mathbf{r}/r$, and $\hat{z}$ is the unit vector in z direction, perpendicular to 2DEG. The definition of $\mathbf{a}$ in a more general case is given in [40]. It should be emphasized that the spin-orbit interaction is the origin of the spin polarization rotations described by Eq. (13). The short-time approximation

was used in the investigation of the spin relaxation dynamics near the edge of 2DEG [41].

3. Anisotropy of spin transport in 2DEG

In some cases the drift-diffusion equations for the spin polarization vector have a rather simple solution. For example, spin dynamics in 2DEG controlled by the spin-orbit interaction, Eqs. (1,2), can be described [37, 40] by Eq. (11). Within the single particle model it is possible to obtain the explicit form of the coefficients $\hat{\mathbf{D}}, \hat{\mathbf{A}}, \hat{\mathbf{C}}$,

$$\hat{\mathbf{D}} = \begin{pmatrix} D & 0 & 0 \\ 0 & D & 0 \\ 0 & 0 & D \end{pmatrix},$$

$$\hat{\mathbf{A}} = \begin{pmatrix} \mu E & 2B_{xz}D & 0 \\ -2B_{xz}D & \mu E & 0 \\ 0 & 0 & \mu E \end{pmatrix}, \tag{14}$$

$$\hat{\mathbf{C}} = \begin{pmatrix} D(B_{xz}^2 + B_{yz}^2) & -\mu E B_{xz} & -B_{yx}B_{yz}D \\ \mu E B_{xz} & D(B_{xz}^2 + B_{yx}^2 + B_{yz}^2) & 0 \\ -B_{yx}B_{yz}D & 0 & DB_{yx}^2 \end{pmatrix},$$

where D and μ are the diffusion coefficient and the mobility of the carriers; B_{ij} describes effects of the spin-orbit interaction and is a function of the spin-orbit coupling coefficients α and β. The spin evolution is characterized by the dissipation of the spin polarization due to random motion of carriers and coherent spin precession. The symmetry of the first mechanism is specified by the geometry of the structure, while the latter is determined by the direction of external electric field. The spin dynamics in such a system can be strongly anisotropic [14, 46]. For example, for a quantum well grown in the (001) direction, if spin-orbit coupling constants α and β are equal the spin dissipation is suppressed for electrons propagating along the $(1\bar{1}0)$ direction. For an arbitrary orientation of the electron transport, and $\alpha = \beta$, the solution for the spin polarization density in an appropriately selected [37] coordinate system can be represented as

$$
\begin{aligned}
P_x &= P_x^0 e^{-\left(\frac{\mu E}{2D}+\sqrt{\left(\frac{\mu E}{2D}\right)^2+B_{yz}^2}\right)x} \cos\left(B_{xz}x\right), \\
P_y &= P_y^0 e^{-\left(\frac{\mu E}{2D}+\sqrt{\left(\frac{\mu E}{2D}\right)^2+B_{yz}^2}\right)x} \sin\left(B_{xz}x\right), \\
P_z &= P_z^0 e^{-\frac{\mu E}{D}x},
\end{aligned}
\tag{15}
$$

where the angular dependence is hidden in the coefficients B_{ij}. In this case the z-component of the spin polarization density is not affected by the spin-orbit interaction, while x and y components experience coherent damped oscillations. The spin precession length, $L_p = 2\pi/B_{xz}$, and the spin dephasing length,

$$
L_\perp = \left(\frac{\mu E}{2D} + \sqrt{\left(\frac{\mu E}{2D}\right)^2 + B_{yz}^2}\right)^{-1}, \tag{16}
$$

are shown in Fig. 2 for a 10 nm AlGaAs/GaAs/AlGaAs quantum well, as functions of the orientation with respect to the (100) crystallographic direction. For the orthogonal component of the spin polarization density, $P_\perp$, spin dephasing is suppressed if the applied electric field is along the $(1\bar{1}0)$ direction. The frequency of the coherent spin precession is maximal in this case. For transport in the (110) direction, spin dephasing is maximal and the frequency of the oscillations is zero. The in-plain electric field in this case affects the spin dephasing mechanism only. Similar dependence of spin dephasing on the electric field has been found in many other applications [31, 45, 47].

III. KINETIC EQUATIONS

For spin-polarized transport, it is possible to derive Boltzmann like kinetic equations by using density matrix approach [49], non-equilibrium Green functions [50, 51] or Wigner functions [37, 52]. All of these approaches allow accounting of additional spin-dependent terms starting from quantum mechanical equations. For example, the Wigner function equation for non-interacting spin polarized electrons in a semiconductor heterostructure can be derived using a single-electron Hamiltonian in the effective mass approximation. For the one subband transport, the Hamiltonian is

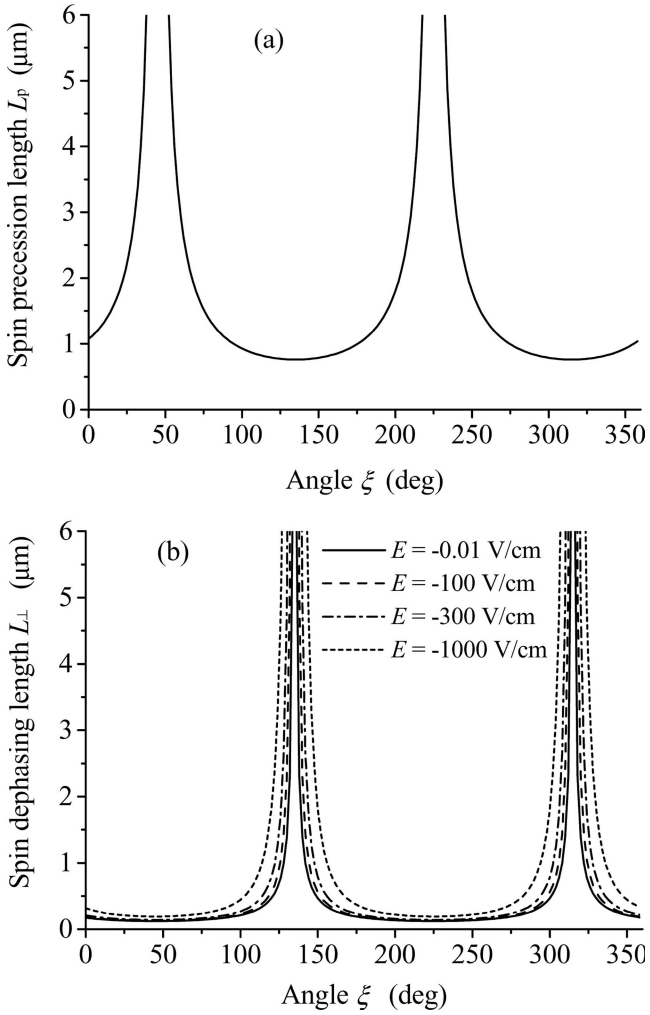

FIG. 2: Spin precession length (a), and transverse spin dephasing length (b), for different transport orientations with respect to the (001) crystallographic direction, at room temperature.

$$H = \frac{\mathbf{p}^2}{2m^*} + V(\mathbf{r}) + H_{\rm SO}, \tag{17}$$

$$H_{\rm SO} = \mathbf{p}\mathbf{A}\sigma/\hbar, \tag{18}$$

where spin-orbit interaction terms, Eqs. (1,2), are written in a dyadic form. Based on Eq. (17), and following the standard transformation to the Wigner function [53],

$$W_{ss'}(\mathbf{R},\mathbf{k},t)=\int \rho(\mathbf{R},\Delta\mathbf{r},s,s',t)e^{-i\mathbf{k}\Delta\mathbf{r}}d^2\Delta r, \tag{19}$$

and also assuming that the potential, $V(\mathbf{r})$, varies slowly and smoothly with coordinates, the transport equation will be [37, 52]

$$\frac{\partial W}{\partial t}+\frac{1}{2}\left\{v_j,\frac{\partial W}{\partial x_j}\right\}-\frac{1}{\hbar}\frac{\partial V}{\partial x_j}\frac{\partial W}{\partial k_j}+ik_j\left[v_j,W\right]=\mathrm{St}W. \tag{20}$$

At the right hand side of Eq. (20) we have included the phenomenological scattering term, StW, responsible for interactions of an electron with phonons and impurities. In the spinor space, the velocity operator components, v_i, and the Wigner function, W, are 2×2 matrixes, while the potential, $V(\mathbf{r})$, and the electron wave vector components, k_i, are proportional to the unit matrix. The scattering term can be rather complicated including a mixture of different spin components [51]. The matrix equation (20) can be projected to the set of Pauli matrixes plus the unit matrix to obtain four coupled equations [37, 52]. Usually, analytical solution of spin polarized transport equations can be found for very simple cases only [52]. For transport regime close to equilibrium a solution can be found using an iteration procedure [49] or a moment expansion scheme [37, 50]. If the transport regime is far from equilibrium or the electron-electron spin exchange interaction needs to be included, numerical solution schemes [51, 54] have to be utilized.

IV. MONTE CARLO MODELING

Monte Carlo device simulation is a widely used method for modeling charge carrier transport in semiconductor structures and devices [55]. It is particularly well suited for highlighting the leading physical mechanisms and studying the transport characteristics. Moreover, it can yield an accurate description of electronic devices. With given material properties of the semiconductor, it can account for non-equilibrium phenomena of charge carrier transport in the device channel and provide resolution beyond the drift-diffusion and hydrodynamic models. The step-wise simulation feature of the Monte Carlo approach makes it easier to accommodate different properties of the electron transport and device design in the simulation. However, the model is rather time consuming. Therefore, in device simulation it is used, usually, to extract physical parameters required as the input data for macroscopic drift-diffusion or hydrodynamic models.

The conventional Monte Carlo scheme describes transport of classical particles. In simulation the particles propagate along classical "localized" trajectories with the averaged momentum during the time interval which is the smaller of the scattering time or sampling time. The propagation momentum is set equal to the average value of the momentum of a particle moving with constant acceleration during this time interval. The scattering events are determined by defects, phonons, device geometry, etc., and are instantaneous. The scattering rates are given by the Fermi's golden rule. Usually, each simulated particle represents many real electrons or holes. The Coulomb interaction between particles can be accounted for within the mean field approximation, by solving the Poisson equation at every sampling time step.

In most of published schemes for spin polarized transport [56–62] the spin dynamics is incorporated into the conventional Monte Carlo approach. If spin-dependent interactions between the particles in the system are small, then each spin can be considered separately driven by an external force or controlled by the spatial motion. In reverse, spin dynamics will also affect the spatial transport characteristics. The later effect is typically small and can be included as a classical force acting on the particles, or even neglected. In simulations, the spin property can be described by a binary up-down parameter, single spin density matrix or spin polarization vector.

A. Physical phenomena simulation

Generally, simulations of spin-related phenomena in semiconductor heterostructures within the standard Monte Carlo approaches require a lot of computational resources. However, there are situations when the knowledge of the result with a high precision is not required. For example, simplified simulation schemes were found to be useful in modeling of physical phenomena. Let us present a Monte Carlo approach based on simplified consideration of the electron spatial motion, with density-matrix approach to the electron spin. This approach was successfully used for studies of spin relaxation in 2DEG with an antidot lattice [61], dynamics of spin relaxation near the edge of the 2DEG [41], control of spin polarization by pulsed magnetic fields [60], and investigation of long-lived spin coherence states [62]. Several examples of application of this approach are given below.

1. Method

A simplified Monte Carlo approach suitable for physical phenomena simulations was introduced in [57]. Within the Monte Carlo simulation algorithm, the space motion of 2DEG electrons is considered to be along classical (linear) trajectories interrupted by the bulk scattering events. The modeling involves spin-independent bulk scattering processes, which could be caused, e.g., by phonon scatterings or impurities. For the sake of simplicity, the scattering due to such events is assumed to be elastic and isotropic, i.e., the magnitude of the electron velocity is conserved in the scattering events, while the final direction of the velocity vector is randomly selected. The time scale of the bulk scattering events can then be fully characterized by a single rate parameter, the momentum relaxation time, τ_p. It is connected to the mean free path by $L_p = v\tau_p$. Here v is the mean electron velocity.

In simulations, the electron spin polarization is conveniently described by the spin polarization vector $\mathbf{P}$. Usually, the spin Hamiltonian consists solely of the spin-orbit terms. It is possible to assume that spin-orbit interactions influence only the spin coordinate, while the reciprocal effect of the spin on the electron spatial motion can be neglected. Phenomenologically, the effect of the spin-orbit couplings can be regarded as an effective magnetic field. In the presence of a magnetic field, the electron spin feels a torque and precesses in the plane perpendicular to the magnetic field direction with an angular frequency. Momentum scattering reorients the direction of the precession axis, making the orientation of the effective magnetic field random and trajectory-dependent, thus leading to an average spin relaxation (dephasing). The quantum mechanical evolution of $\mathbf{P}$ can be conveniently described by the classical equation of motion [57]. In 2DEG with Rashba spin-orbit interaction this effective magnetic field can be conveniently described by a single parameter η that is the electron spin precession angle per unit length.

At the initial moment of time the electron coordinates and direction of velocity are randomly generated, while the spin direction is selected according to initial conditions. The main loop of the Monte Carlo simulation algorithm involves the following steps: generation of a time interval between two consecutive scattering events, calculation of the spin dynamics (using the spin polarization vector equation of motion), and random generation of a new direction of the electron velocity after scattering. Consecutive applications of these operations allow finding the electron position and spin direction at any arbitrary moment of time. Normally, the spin polarization is calculated as a function of time and coordinate by averaging over an ensemble of $10^7 \div 10^9$ electrons. The spin relaxation time can be

evaluated by fitting the time dependence to an exponential decay.

2. Relaxation of electron spin polarization in 2DEG with antidot lattice

Long spin relaxation times are desirable for spintronic device operation. Recently, the use of a two-dimensional electron system, for example, 2DEG in an heterostructure, with a lattice of antidots, was proposed for spintronic device engineering [61]. In this model, electrons move semiclassically in a plane containing reflecting disks (antidots) of radius r, centered at the sites of a square lattice with lattice spacing a, as shown in Fig. 3(a). Lattice of antidots can be formed when, e.g., a periodic array of holes is etched into the top layers of a semiconductor heterostructure by means of conventional fabrication. Based on experimental results, we consider the D'yakonov-Perel' (DP) mechanism [63] to be the dominant spin relaxation channel. Using a Monte Carlo simulation scheme originally proposed in [57], the electron spin relaxation time due to the DP mechanism was calculated, for different values of spacing between the antidot centers, the antidot radius, and the strength of the spin-orbit interaction. An interesting pattern of dependence of the spin relaxation time on the geometrical parameters of the antidot lattice was discovered. These results are presented below.

Figure 3(b) shows the calculated spin relaxation time as a function of antidot radius for several fixed values of a. The behavior of the spin relaxation time can be classified in three different regimes. For small r, the dependence is not exponential. Increase of the electron spin relaxation time in this regime is most pronounced for small a; see the top curve in Fig. 3(b). Next there follows the regime where the r-dependence of the spin relaxation time is approximately exponential, see the straight line fits on Fig. 3(b). This dependence is valid over almost half of the range of change of the antidot radius, approximately for $0.1 < r/a < 0.35$. For larger r, we observe transition to non-exponential behavior or possibly to an exponential behavior with different slope.

These results were also compared with the results of a Monte Carlo simulation made with the assumption of "rough" antidots, for which we choose the angle of motion of an electron after scattering from an antidot randomly, in $[-\pi/2, \pi/2]$ from the radial direction. As illustrated in Fig. 3(b), the spin relaxation time is then only slightly longer than the spin relaxation time with the same system parameters for the reflecting antidots and has almost the same dependence on the antidot radius. This increase in the spin relaxation time likely arises from additional randomization of the electron spatial trajectory by "rough" scattering events.

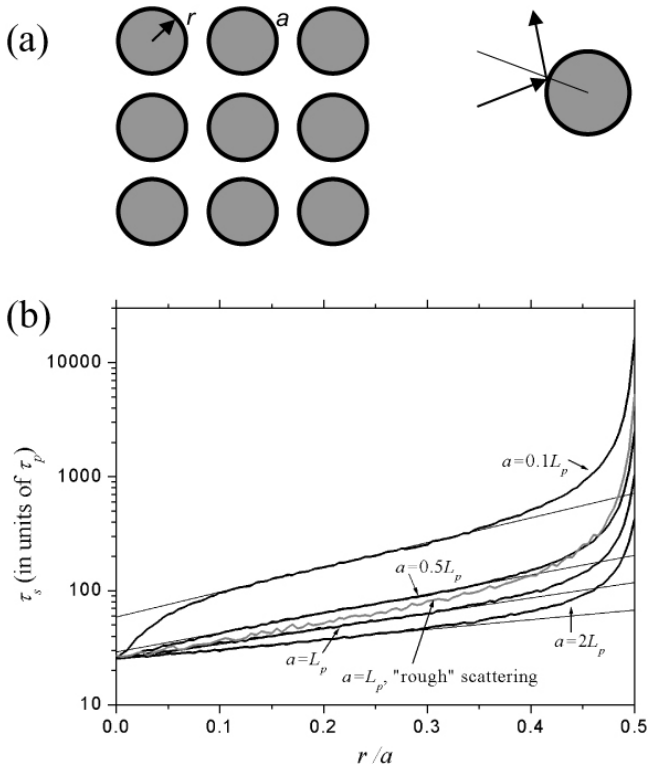

FIG. 3: (a) The antidot lattice. (b) Electron spin relaxation time, τ_s, as a function of the antidot radius, for different spacing between the antidots, with $\eta L_p = 0.2$. The straight lines are the fitted exponentials; τ_p is the momentum relaxation time. The spin relaxation time has finite values at $r = 0.5a$.

3. Long-living spin coherence states

Traditionally, investigations of electron spin relaxation in two-dimensional semiconductor heterostructures at zero applied electric field have focused either on properties of spatially homogeneous or spatially inhomogeneous spin polarization but with the same direction of the spin polarization vector. In the recent paper [60], the effect of the initial distribution of direction of the spin polarization on spin lifetime for electrons in quantum wells was studied. The system under investigation consists of electrons in 2DEG with specific orientation of the electron spins at initial moment of time. Specifically, the spin dynamics of two initial spin configurations, namely a spin polarization strip and a novel structure—spin coherence standing wave, were studied. In the spin coherence standing wave, the initial direction of spin polarization is a periodic function of coordinate. It was show that such a structure is more robust against relaxation than the electron

spin polarization having the same direction of spin polarization vector.

Let us consider the evolution of non-equilibrium spin polarization in 2DEG with Rashba spin-orbit interaction. The initial direction of the spin polarization in the spin coherence standing wave, see Fig. 4(a), is a periodic function of x with the components $(-S_0 \sin(2\pi x/a), 0, S_0 \cos(2\pi x/a))$, where S_0 is the amplitude and a is the wavelength (period) of the spin coherence standing wave. Monte-Carlo simulation algorithm [57] was used in studies of dynamics of this structure. Fig. 4(b) shows the component and amplitude of the spin coherence standing wave at $t = 5\tau_p$. It was found [62] that in the central region the amplitude of spin coherence standing wave is a periodic function of x with minima corresponding to maxima of S_x and with maxima corresponding to maxima of S_z. We attribute the transition from a constant spin polarization amplitude at $t = 0$ to a periodic one at subsequent times to the dependence of the spin relaxation times on the initial direction of the spin polarization vector. It is well known that the spin relaxation time of in-plane spin polarization is two times longer then the spin relaxation time of the spin polarization perpendicular to plane [63].

Spin relaxation time of the spin coherence standing wave as a function of its period is depicted in Fig. 4(c). This dependence has a maximum exactly at $a = 2\pi/\eta$. The data presented in Fig. 4(c) indicate that the spin relaxation time of the spin coherence standing wave is longer than the spin relaxation time of homogeneous spin polarization. At the maximum, the relaxation time is 6 times as large for the spin coherence standing wave as for the homogeneous spin polarization in the z direction. This increase of spin relaxation time can be explained by suppression of spin dephasing during diffusion in the x direction. It should be pointed out that the spin relaxation only due to the D'yakonov-Perel' mechanism was suppressed. Other relaxation mechanism could be important. We can list the following possible relaxation mechanisms: Elliot-Yafet [64], Bir-Aronov-Pikus [65], relaxation due to fluctuations of the spin-orbit interaction [66], and relaxation by nuclear spins [67]. Another possible source of spin dephasing is a many body mechanism proposed by Wu [68]. However, the joint action of these mechanisms was not studied.

B. Device simulation

To study spin-polarized transport in a device structure the simulation model can be rather complicated including detailed models of scattering, multi-valley and multi-subband transport, electron-electron interactions, etc. Broad classes of spin-related phenomena, e.g., temperature and field effects on spin dynamics

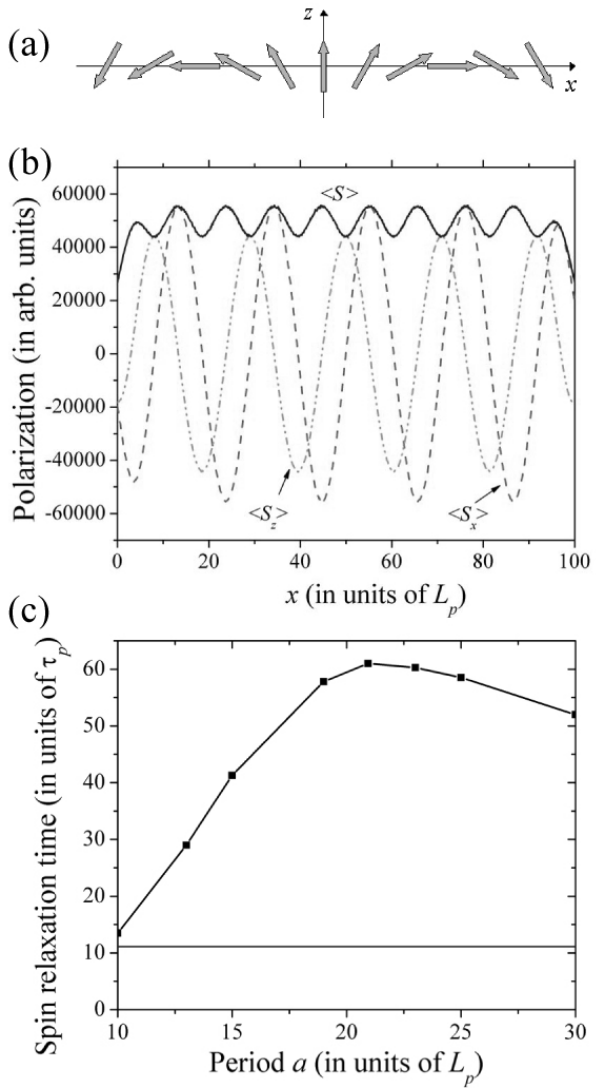

FIG. 4: (a) Schematics of the spin coherence standing wave: direction of the spin polarization vector is indicated by the arrows. (b) Total polarization and polarization components of the spin coherence standing wave at $t = 5\tau_p$, $a = 20.94L_p$ and $\eta L_p = 0.3$. (c) Dependence of the electron spin relaxation time on the spin coherence standing wave period. The straight line shows the spin relaxation time of homogeneous spin polarization in the same system. This plot was obtained using the parameter value $\eta L_p = 0.3$.

[58, 59], spin noise [69], symmetry of spin scattering mechanisms [70], can be addressed using such a model. As an example, we consider here the problem of spin injection through a Schottky barrier at the metal/2D-semiconductor interface.

At the present time, electric spin injection from a ferromagnetic metal into a non-magnetic semiconductor through a tunneling barrier is most promising for device applications. It resolves conductivity mismatch problem [71] and allows spin injection at room temperature. Such a design has been utilized, for example, in Spin-LEDs [72].

In a simulation model the Schottky barrier profile can be calculated based on the electron concentration in a semiconductor with boundary conditions specified by the applied voltage [73]. Initially, electrons in semiconductor are non-polarized, while spin polarization of electrons in the metal contact is given. Spin-polarized electrons are transported into the semiconductor by two different mechanisms, thermionic emission and tunneling. Both mechanisms can be accounted for in the Monte Carlo model [74, 75]. Single-particle spin dynamics in semiconductor due to spin dependent interaction H_{S} can be described using the density matrix,

$$\rho(t+\Delta t) = e^{-iH_{\mathrm{S}}\Delta t/\hbar}\rho(t)e^{iH_{\mathrm{S}}\Delta t/\hbar}, \tag{21}$$

where Δt is the sampling time or the time interval between two scattering events. Additional spin scattering can be included during the momentum scattering events. Injected spin-polarized electrons represent only a small fraction of electrons in the semiconductor part. In this case it is better to use two types of representative particles in a Monte Carlo scheme [73]. Moreover, to study spin dynamics, statistical averaging should be carried out over one type of particles only (injected or persistently existing in the device channel). In [74, 75] we have utilized the current spin polarization

$$P_{\sigma_\alpha}^{J_\beta} = J_{\sigma_\alpha}^{\beta} / J_\beta, \tag{22}$$

where J_β is a β component of the current density, and the spin current density J_σ^β is defined as

$$J_{\sigma_\alpha}^{\beta} = \sum_i v_\beta^i Tr(\sigma_\alpha \rho_i). \tag{23}$$

This parameter naturally separates the injected spin-polarized electrons from the non-polarized background electrons. The simulations show that the electrons injected through the barrier are not thermalized. In that case, the drift-diffusion

model is hardly applicable and more sophisticated analytical approaches, like an energy transport model or hydrodynamic model [76] should be used.

In summary, in this short review we have discussed several models widely accepted for spin-polarized transport in semiconductor structures. These models provide a means for simulating spin-related processes with different levels of complexity and precision. Applications were illustrated on several examples.

ACKNOWLEDGMENTS

We gratefully acknowledge helpful discussions with M.-C. Cheng, M. Shen and I. D. Vagner. This research was supported by the National Security Agency and Advanced Research and Development Activity under Army Research Office contract DAAD-19-02-1-0035, and by the National Science Foundation, grant DMR-0121146.

---

[1] S. A. Wolf, D. D. Awschalom, R. A. Buhrman, J. M. Daughton, S. von Molnar, M. L. Roukes, A. Y. Chtchelkanova, D. M. Treger, Science **294**, 1488 (2001).

[2] I. Žutić, J. Fabian, S. Das Sarma, Rev. Mod. Phys. **76**, 323 (2004).

[3] H. Akinaga, H. Ohno, IEEE Transactions on Nanotechnology **1**, 19 (2002).

[4] J. F. Gregg, I. Petej, E. Jouguelet, C. Dennis, J. Phys. D: Appl. Phys. **35**, R121 (2002).

[5] S. Das Sarma, Am. Sci. **89**, 516 (2001).

[6] D. D. Awschalom, M. E. Flatté, N. Samarth, Sci. Am. **286**, 66 (2002).

[7] Research Needs for Novel Devices (SRC, May 2003).

[8] S. Datta, B. Das, Appl. Phys. Lett. **56**, 665 (1990).

[9] R. G. Mani, W. B. Johnson, V. Narayanamurti, V. Privman, Y. H. Zhang, Physica E **12**, 152 (2002).

[10] X. F. Wang, P. Vasilopoulos, F. M. Peeters, Appl. Phys. Lett. **80**, 1400 (2002).

[11] M. Governale, D. Boese, U. Zulicke, C. Schroll, Phys. Rev. B **65**, 140403 (2002).

[12] R. Vrijen, E. Yablonovitch, K. Wang, H. W. Jiang, A. Balandin, V. Roychowdhury, T. Mor, D. DiVincenzo, Phys. Rev. A **62**, 012306 (2000).

[13] J. Schliemann, J. C. Egues, D. Loss, Phys. Rev. Lett. **90**, 146801 (2003).

[14] J. C. Egues, G. Burkard, D. Loss, Appl. Phys. Lett. **82**, 2658 (2003).

[15] K. C. Hall, W. H. Lau, K. Gundogdu, M. E. Flatté, T. F. Boggess, Appl. Phys. Lett. **83**, 2937 (2003).

[16] M. E. Flatté, Z. G. Yu, E. Johnson-Halperin, D. D. Awschalom, Appl. Phys. Lett. **82**, 4740 (2003).
[17] J. Fabian, I. Žutić, S. Das Sarma, Appl. Phys. Lett. **84**, 85 (2004).
[18] S. Bandyopadhyay, M. Cahay, e-print cond-mat/0408137.
[19] B. Wang, J. Wang, H. Guo, Phys. Rev. B **67**, 092408 (2003).
[20] C. Ciuti, J. P. McGuire, L. J. Sham, Appl. Phys. Lett. **81**, 4781 (2002).
[21] S. Parkin, X. Jiang, C. Kaiser, A. Panchula, K. Roche, M. Samant, Proc. IEEE **91**(5), 61 (2003).
[22] M. I. Dyakonov , talk presented at the Future Trends in Microelectronics workshop, Corsica, June 2003, e-print cond-mat/0401369.
[23] S. Bandyopadhyay, M. Cahay, e-print cond-mat/0404339.
[24] Y. Ohno, R. Terauchi, T. Adachi, F. Matsukura, H. Ohno, Phys. Rev. Lett. **83**, 4196 (1999).
[25] O. Z. Karimov, G. H. John, R. T. Harley, W. H. Lau, M. E. Flatté, M. Henini, R. Airey, Phys. Rev. Lett. **91**, 246601 (2003).
[26] I. Malajovich, J. J. Berry, N. Samarth, D. D. Awschalom, Nature **411**, 770 (2001).
[27] J. M. Kikkawa, D. D. Awschalom, Nature **397**, 136 (1999).
[28] M. J. Stevens, A. L. Smirl, R. D. R. Bhat, A. Najmaie, J. E. Sipe, H. M. van Driel, Phys. Rev. Lett. **90**, 136603 (2003).
[29] G. Dresselhaus, Phys. Rev. **100**, 580 (1955).
[30] E. I. Rashba, Fiz. Tverd. Tela (Leningrad) **2**, 1224 (1960) [Sov. Phys. Solid State **2**, 1109 (1960)]. Y. A. Bychkov, E. I. Rashba, J. Phys. C **17**, 6039 (1984).
[31] Z. G. Yu, M. E. Flatté, Phys. Rev. B **66**, 235302 (2002); Z. G. Yu, M. E. Flatté, Phys. Rev. B **66**, 201202 (2002).
[32] I. Žutić, J. Fabian, S. Das Sarma, Phys. Rev. Lett. **88**, 066603 (2002).
[33] Yu. V. Pershin, V. Privman, Phys. Rev. Lett. **90**, 256602 (2003).
[34] Yu. V. Pershin, V. Privman, Proc. Conference "IEEE-NANO 2003" (IEEE Press, Monterey, CA, 2003), p. 168.
[35] Yu. V. Pershin, Phys. Rev. B **68**, 233309 (2003).
[36] I. Martin, Phys. Rev. B **67**, 014421 (2003).
[37] S. Saikin, J. Phys.: Condens. Matter **16**, 5071 (2004)
[38] E. Shafir, M. Shen, S. Saikin, e-print cond-mat/0407416.
[39] D. Culcer, J. Sinova, N. A. Sinitsyn, T. Jungwirth, A. H. MacDonald, Q. Niu, Phys. Rev. Lett. **93**, 046602 (2004).
[40] Yu. V. Pershin, Physica E **23**, 226 (2004).
[41] Yu. V. Pershin, e-print cond-mat/0406064.
[42] A. A. Burkov, Alvaro S. Nunez, A. H. MacDonald, cond-mat/0311328 (unpub-

lished).
[43] N. F. Mott, Proc. Roy. Soc. (London) Ser. A **153**, 699 (1936).
[44] A. Fert, I. A. Campbell, J. Physique (Paris) Colloq. **32**, C1-46 (1971).
[45] A. G. Aronov, G. E. Pikus, Sov. Phys. Semicond. **10**, 698 (1976) [Fiz. Tekh. Poluprovodn. **10**, 1177 (1976)].
[46] N. S. Averkiev, L. E. Golub, Phys. Rev. B **60**, 15582 (1999).
[47] Y. Qi, S. Zhang, Phys. Rev. B **67**, 052407 (2003).
[48] G. E. W. Bauer, Y. Tserkovnyak, D. Huertas-Hernando, A. Brataas, From Digital to Analogue Magnetoelectronics: Theory of Transport in Non-collinear Magnetic Nanostructures, *in Advances in Solid State Physics*, vol. 43 (Springer-Verlag, Berlin 2003).
[49] E. L. Ivchenko, Yu. B. Lyanda-Geller, G. E. Pikus, Sov. Phys. JETP **71**, 550 (1990), [Zh. Eksp. Teor. Fiz. **98**, 989 (1990)].
[50] Y. Takahashi, K. Shizume, N. Masuhara, Phys. Rev. B **60**, 4856 (1999).
[51] M. Q. Weng, M. W. Wu, J. Appl. Phys. **93**, 410 (2003).
[52] E. G. Mishchenko, B. I. Halperin, Phys. Rev. B **68**, 045317 (2003).
[53] E. Wigner, Phys. Rev. **40**, 749 (1932).
[54] M. Q. Weng, M. W. Wu, L. Jiang, Phys. Rev. B **69**, 245320 (2004).
[55] K. Hess, Monte Carlo Device Simulation: Full Band and Beyond (Kluwer Academic Publishers, Boston, 1991).
[56] A. Bournel, P. Dollfus, E. Cassan, P. Hesto, Appl. Phys. Lett. **77**, 2346 (2000).
[57] A. A. Kiselev, K. W. Kim, Phys. Rev. B **61**, 13115 (2000).
[58] S. Saikin, M. Shen, M.-C. Cheng, V. Privman, J. Appl. Phys. **94**, 1769 (2003).
[59] S. Pramanik, S. Bandyopadhyay, M. Cahay, Phys. Rev. B **68**, 075313 (2003).
[60] Yu. V. Pershin, e-print cond-mat/0310225.
[61] Yu. V. Pershin, V. Privman, Phys. Rev. B **69**, 073310 (2004).
[62] Yu. V. Pershin, e-print cond-mat/0311223.
[63] M. I. D'yakonov, V. I. Perel', Sov. Phys. Solid State **13**, 3023 (1972); M. I. Dyakonov, V. Y. Kachorovskii, Sov. Phys. Semicond. **20**, 110 (1986).
[64] P. G. Elliott, Phys. Rev. 96, 266 (1954); Y. Yafet, Solid State Phys. **14**, 1 (1963).
[65] G. L. Bir, A. G. Aronov, G. E. Pikus, Zh. Eksp. Teor. Fiz. **69**, 1382 (1975) [Sov. Phys. JETP **42**, 705 (1976)].
[66] E. Ya. Sherman, Phys. Rev. B **67**, 161303 (R) (2003); E. Ya. Sherman, Appl. Phys. Lett. **82**, 209 (2003).
[67] Yu. V. Pershin, V. Privman, Nano Lett. **3**, 695 (2003).
[68] M. Q. Weng, M. W. Wu, Phys. Rev. B **66**, 235109 (2002); M. Q. Weng, M. W. Wu, Phys. Rev. B **68**, 075312 (2003).

[69] S. Pramanik, S. Bandyopadhyay, cond-mat/0312099 (Presented at the International Symposium on Clusters and Nano-Assemblies, Richmond, VA, USA, November 2003).

[70] S. Saikin, M. Shen, M.-C. Cheng, IEEE Trans. Nanotechnology **3**, 173 (2004).

[71] G. Schmidt, D. Ferrand, L. W. Molenkamp, A. T. Filip, B. J. van Wees, Phys. Rev. B **62**, R4790 (2000).

[72] A. T. Hanbicki, O. M. J. van 't Erve, R. Magno, G. Kioseoglou, C. H. Li, B. T. Jonker, G. Itskos, R. Mallory, M. Yasar, A. Petrou, App. Phys. Lett. **82**, 4092 (2003).

[73] M. Shen, M.-C. Cheng (unpublished).

[74] M. Shen, S. Saikin, M.-C. Cheng, J. Appl. Phys., in press, e-print cond-mat/0405270.

[75] M. Shen, S. Saikin, M.-C. Cheng, IEEE Trans. Nanotechnology, in press, e-print cond-mat/0405591.

[76] C. Timm, F. von Oppen, F. Hofling, Phys. Rev. B **69**, 115202 (2004).